Acta Cryst
E
CRYSTALLOGRAPHIC
COMMUNICATIONS

ISSN 2056-9890

Glycine zinc sulfate pentahydrate: redetermination at 10 K from time-of-flight neutron Laue diffraction

A. Dominic Fortes,[a]* Christopher M. Howard,[b] Ian G. Wood[b] and Matthias J. Gutmann[a]

[a]ISIS Facility, Rutherford Appleton Laboratory, Harwell Science and Innovation, Campus, Didcot, Oxfordshire OX11 0QX, England, and [b]Department of Earth Sciences, University College London, Gower Street, London, WC1E 6BT, England. *Correspondence e-mail: dominic.fortes@stfc.ac.uk

Received 11 August 2016
Accepted 8 September 2016

Edited by M. Weil, Vienna University of Technology, Austria

Keywords: crystal structure; glycine; zinc sulfate; zwitterion; dimer; neutron diffraction.

CCDC reference: 1503478

Supporting information: this article has supporting information at journals.iucr.org/e

Single crystals of glycine zinc sulfate pentahydrate [systematic name: hexaaquazinc tetraaquadiglycinezinc bis(sulfate)], $[Zn(H_2O)_6][Zn(C_2H_5NO_2)_2(H_2O)_4](SO_4)_2$, have been grown by isothermal evaporation from aqueous solution at room temperature and characterized by single-crystal neutron diffraction. The unit cell contains two unique ZnO_6 octahedra on sites of symmetry $\overline{1}$ and two SO_4 tetrahedra with site symmetry 1; the octahedra comprise one [tetraaqua-diglycine zinc]$^{2+}$ ion (centred on one Zn atom) and one [hexaaquazinc]$^{2+}$ ion (centred on the other Zn atom); the glycine zwitterion, $NH_3^+CH_2COO^-$, adopts a monodentate coordination to the first Zn atom. All other atoms sit on general positions of site symmetry 1. Glycine forms centrosymmetric closed cyclic dimers due to $N-H\cdots O$ hydrogen bonds between the amine and carboxylate groups of adjacent zwitterions and exhibits torsion angles varying from ideal planarity by no more than 1.2°, the smallest values for any known glycine zwitterion not otherwise constrained by a mirror plane. This work confirms the H-atom locations estimated in three earlier single-crystal X-ray diffraction studies with the addition of independently refined fractional coordinates and U_{ij} parameters, which provide accurate internuclear $X-H$ (X = N, O) bond lengths and consequently a more accurate and precise depiction of the hydrogen-bond framework.

1. Chemical context

Numerous coordination compounds of glycine (Glyc) with divalent metal sulfates are known. For the case of zinc, there is an anhydrous species, $2Glyc\cdot ZnSO_4$ (Moldobaev & Nogoev, 1970) and two hydrates, $Glyc\cdot ZnSO_4\cdot 3H_2O$ and $Glyc\cdot ZnSO_4\cdot 5H_2O$. The trihydrate is dimorphic, occurring either as an orthorhombic crystal (space group $Pca2_1$) or as a monoclinic crystal ($P2_1/n$) depending on the synthesis route (Fleck & Bohatý, 2004). The monoclinic form is isotypic with compounds of general formula $Glyc\cdot M(II)SO_4\cdot 3H_2O$ where M(II) = Mg, Co or Fe (Oguey *et al.*, 2013*a*,*b*, 2014). Compounds with the general formula $Glyc\cdot M(II)SO_4\cdot 5H_2O$ are known only as isotypic triclinic crystals ($P\overline{1}$) for M(II) = Mg, Mn, Co, Fe and Zn (Lindqvist & Rosenstein, 1960; Elayaraja *et al.*, 2007; Fleck & Bohatý, 2006; Tepavitcharova *et al.*, 2012). Solubility data have been published for a purported $Glyc\cdot NiSO_4\cdot 5H_2O$ (Moldobaev *et al.*, 1970; Alymkulova & Salyeva, 1987). We have collected as-yet unpublished X-ray powder-diffraction data from this species, showing that it is isotypic with the other known members of the series. The existence of $Glyc\cdot CuSO_4\cdot 5H_2O$ has been reported by Thilagavathi *et al.* (2012) but their work is in error, and quite unambiguously describes the well-known material $CuSO_4\cdot 5H_2O$.

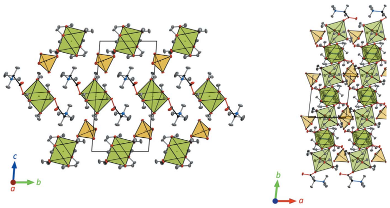

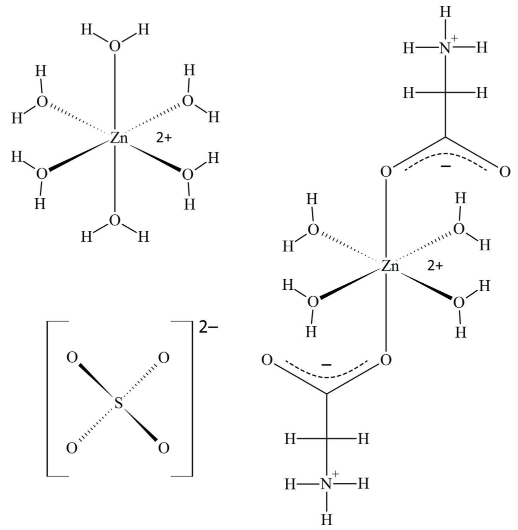

We recently carried out the first neutron diffraction study of Glyc·$MgSO_4\cdot3H_2O$ and Glyc·$MgSO_4\cdot5H_2O$ using perdeuterated powder specimens (Howard *et al.*, 2016). Glyc·$MgSO_4\cdot5H_2O$ tends to form masses of crystals that are both of poor quality and are too small for single-crystal neutron diffraction study; however, this is not the case for Glyc·$MnSO_4\cdot5H_2O$ and Glyc·$ZnSO_4\cdot5H_2O$, where fine tabular to blocky single crystals with volumes substantially in excess of 10 mm^3 are formed with ease (Fig. 1). The objective of this work was to carry out the first single-crystal *neutron* diffraction study of any Glyc·M(II)$SO_4\cdot5H_2O$ compound, specifically using a specimen with M(II) = Zn.

Optical and mechanical properties of the title compound were reported by Balakrishnan & Ramamurthy (2007), although they incorrectly give the composition as Glyc·$ZnSO_4\cdot7H_2O$. The effect of doping Glyc·$ZnSO_4\cdot5H_2O$ with cobalt is described by El-Fadl & Abdulwahab (2010). Three prior structure refinements from single-crystal X-ray diffraction data have been reported (Balamurugan *et al.*, 2011; Tepavitcharova *et al.*, 2012; Oguey *et al.*, 2013*c*); comparisons with this work are detailed in Section 2.

2. Structural commentary

Although the stoichiometry of the material is accurately reflected in its common name, glycine zinc sulfate pentahydrate, the presence of two symmetry-inequivalent Zn sites means that the crystallographically proper structural composition is the 'double' formula $[Gly\cdot ZnSO_4\cdot5H_2O]_2$, or more precisely $[Zn(H_2O)_6][Zn(H_2O)_4(C_2H_5NO_2)_2](SO_4)_2$; the unit cell contains *one* of these units.

The Zn1 coordination octahedron consists of tetraaquadiglycine zinc(II) with the glycine zwitterion ($NH_3^+CH_2COO^-$) coordinating to Zn by one of the carboxylate oxygen atoms (Fig. 2); the inversion centre results in an all-*trans* configuration for these units. The Zn2 octahedron has the form hexaaquazinc(II); the sulfate tetrahedra are isolated, accepting hydrogen bonds primarily (but not exclusively) from Zn-coordinating water molecules (Fig. 3). The S—O bond lengths (Table 1) reflect the number of hydrogen bonds accepted by each apical oxygen atom with a statistical significance which was not apparent from the powder refinement of Howard *et al.* (2016) but which are in excellent agreement with the single-crystal X-ray study of Tepavitcharova *et al.* (2012).

Bond lengths and angles of the glycine zwitterion agree very well with other determinations of related compounds made by X-ray single-crystal diffraction at higher temperatures and extremely well with the determinations in α-glycine at room temperature by neutron single-crystal diffraction (Jönsson & Kvick, 1972; Power *et al.*, 1976), particularly in respect of their mean N—H bond lengths (1.039 Å) and mean C—H bond lengths (1.090 Å). The glycine zwitterion is remarkably planar, with torsion angles O7—C1—C2—N1 = −1.18 (3)° and O8—C1—C2—N1 = 179.23 (2)°, even by comparison with, for example, glycine nickel bromide tetrahydrate (Fleck & Bohatý, 2005), glycine lithium chromate monohydrate and glycine lithium molybdate (Fleck *et al.*, 2006), where torsion angles are in the range 169–176°. Only in glycine magnesium chloride tetrahydrate,

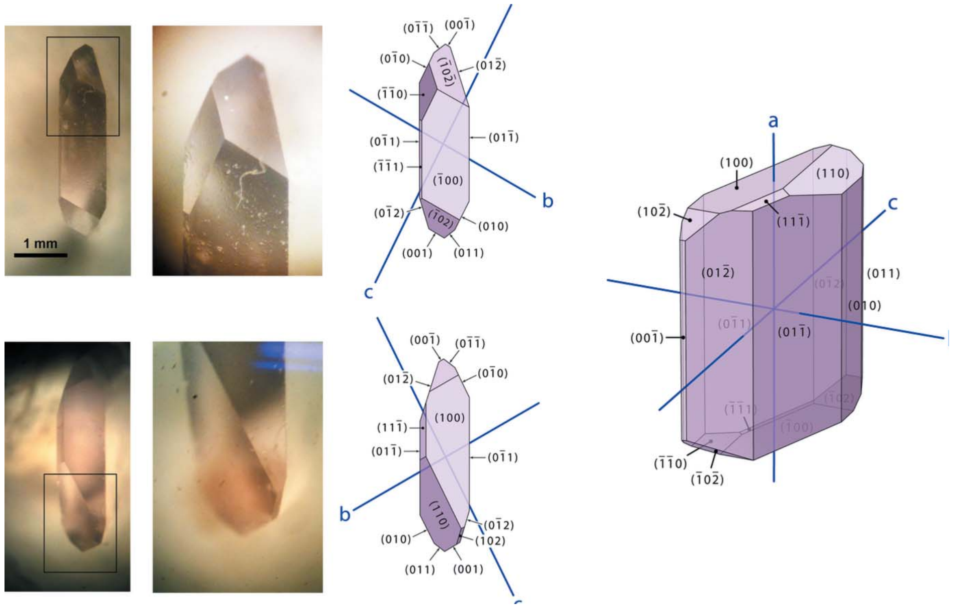

Figure 1
Microphotograph of a representative Glyc·$ZnSO_4\cdot5H_2O$ single crystal viewed along the a axis; insets show details of less well-developed facets (*e.g.*, $\bar{1}11$ and 102). Drawings with each face labelled by the Miller index are shown on the right and a quantitative representation of the model is included in the CIF data. Figure produced and CIF code exported using *WinXMorph* (Kaminsky, 2005, 2007).

Table 1

Comparison of bond lengths (Å), polyhedral volumes (Å^3) and various distortion metrics (*cf.*, Robinson *et al.*, 1971) in Glyc·$ZnSO_4$·$5H_2O$ from this work and the three preceding single-crystal X-ray diffraction studies.

The distortion index and quadratic elongation are dimensionless, whereas the bond-angle variance is in units of degrees squared.

	This work	Balamurugan *et al.* (2011)	Tepavitcharova *et al.* (2012)	Oguey *et al.* (2013*c*)
	Single-crystal neutron *T* = 10 K	Single-crystal X-ray *T* = 293 K	Single-crystal X-ray *T* = 150 K	Single-crystal X-ray *T* = 153 K
S—O1*	1.474 (5)	1.472 (2)	1.472 (1)	1.473 (2)
S—O2	1.484 (4)	1.478 (2)	1.482 (1)	1.485 (2)
S—O3*	1.473 (4)	1.472 (2)	1.477 (1)	1.481 (2)
S—O4	1.480 (5)	1.481 (2)	1.484 (1)	1.479 (2)
Mean S—O	1.478	1.476	1.479	1.479
SO_4 volume	1.656	1.649	1.659	1.661
Distortion index	0.0028	0.0025	0.0027	0.0022
Quadratic elongation	1.000	1.000	1.000	1.000
Bond-angle variance	0.410	0.268	0.320	0.420
Zn1—O5	2.039 (2)	2.024 (3)	2.032 (1)	2.035 (2)
Zn1—O6	2.093 (2)	2.101 (3)	2.098 (1)	2.098 (2)
Zn1—O7†	2.173 (2)	2.181 (3)	2.177 (1)	2.176 (2)
Mean Zn1—O	2.102	2.102	2.102	2.103
ZnO_6 volume	12.338	12.339	12.339	12.336
Distortion index	0.0227	0.0251	0.0238	0.0232
Quadratic elongation	1.003	1.003	1.003	1.003
Bond-angle variance	6.308	4.815	5.975	6.292
Zn2—O9	2.129 (3)	2.141 (3)	2.133 (1)	2.135 (2)
Zn2—O10	2.067 (3)	2.071 (3)	2.070 (1)	2.072 (2)
Zn2—O11	2.075 (2)	2.063 (3)	2.065 (2)	2.065 (2)
Mean Zn2—O	2.090	2.092	2.089	2.091
ZnO_6 volume	12.127	12.176	12.123	12.145
Distortion index	0.0124	0.0156	0.0139	0.0142
Quadratic elongation	1.003	1.002	1.002	1.002
Bond-angle variance	7.982	5.942	6.617	6.541
C1—O7	1.272 (4)	1.272 (5)	1.274 (2)	1.278 (3)
C1—O8	1.240 (3)	1.228 (5)	1.236 (2)	1.234 (3)
C1—C2	1.523 (4)	1.516 (5)	1.525 (3)	1.522 (3)
C2—N1	1.481 (2)	1.478 (5)	1.480 (2)	1.480 (3)

*Denotes sulfate O atoms accepting two hydrogen bonds instead of three. †Denotes carboxylate oxygen ligand instead of water oxygen.

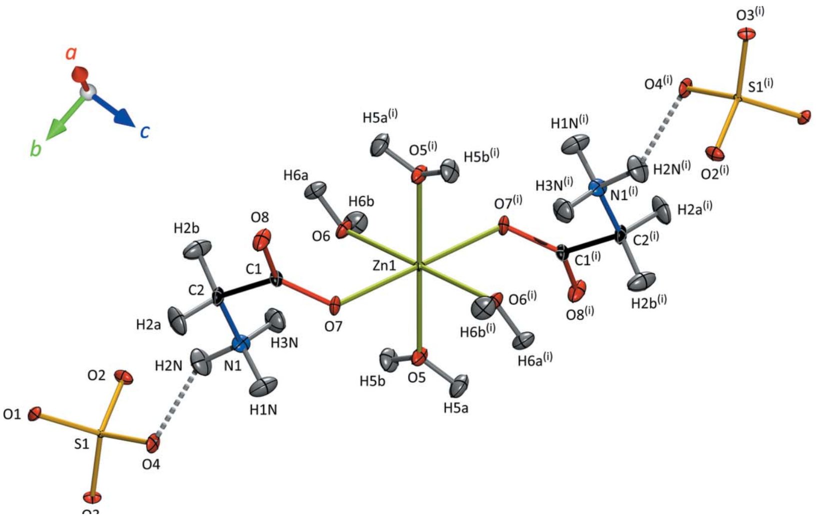

Figure 2

Local coordination environment of the Zn1 atom. Displacement ellipsoids are drawn at the 50% probability level for H and 90% for all other atoms. Dashed lines indicate N—H···O hydrogen bonds. [Symmetry code: (i) $1 - x, -y, 1 - z$.]

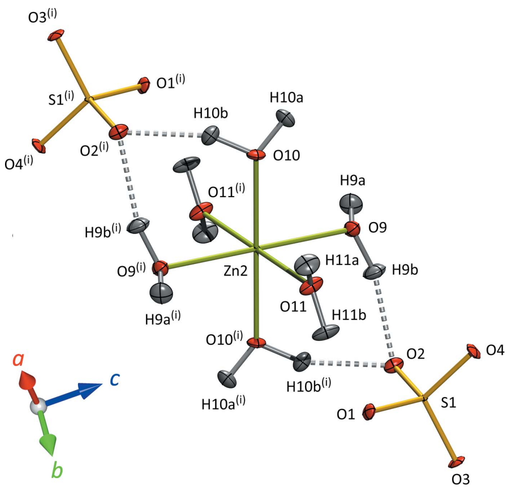

Figure 3

Local coordination environment of the Zn2 atom. Displacement ellipsoids are drawn at the 50% probability level for H and 90% for all other atoms. Dashed lines indicate O—H···O hydrogen bonds. [Symmetry code: (i) $1 - x, -y, 1 - z$.]

Table 2
Comparison of X—H(D) bond lengths (Å) from earlier work (*a*–*e*) with our own (*f*).

Element symbols indicate the cation in each compound. ‘X-ray’ denotes single-crystal X-ray diffraction; ‘NPD’ denotes a neutron powder diffraction experiment on a deuterated analogue carried out at 10 K; ‘neutron’ indicates single-crystal neutron diffraction on a protonated analogue carried out at 10 K. Note that the atom symbols employed in our work are the same as those used by Elayaraja *et al.* (2007) and by Howard *et al.* (2016). Although other authors have used different atom labels – and indeed use them inconsistently in their own reports – we list equivalent contacts in this table.

	Mg, X-ray$^{(a)}$	Mg, NPD$^{(b)}$	Co, X-ray$^{(c)}$	Mg, X-ray$^{(c)}$	Zn, X-ray$^{(c)}$	Zn, X-ray$^{(d)}$	Zn, X-ray$^{(e)}$	Zn, neutron$^{(f)}$
N—H1N	0.87 (4)	1.008 (4)	0.847 (1)	0.849 (1)	0.881 (2)	0.85 (2)	0.910 (2)	1.033 (7)
N—H2N	0.87 (4)	0.982 (4)	0.907 (1)	0.898 (1)	0.904 (1)	0.83 (3)	0.911 (2)	1.028 (8)
N—H3N	0.87 (5)	0.991 (5)	0.904 (1)	0.902 (1)	0.946 (1)	absent	0.910 (2)	1.022 (6)
Average N—H	0.87	0.995	0.877	0.874	0.892	0.84	0.911	1.030
C—H2A	0.970 (4)	1.077 (4)	0.961 (1)	0.960 (1)	0.967 (2)	0.970 (3)	0.990 (2)	1.085 (6)
C—H2B	0.970 (3)	1.083 (4)	0.901 (1)	1.014 (1)	1.050 (2)	0.970 (3)	0.990 (2)	1.091 (7)
Average C—H	0.970	1.080	0.931	0.987	1.009	0.970	0.990	1.088
O5—H5A	0.84 (3)	0.975 (5)	0.880 (1)	0.789 (1)	0.879 (2)	0.85 (2)	0.83 (3)	0.973 (7)
O5—H5B	0.85 (3)	0.946 (5)	0.914 (1)	0.930 (1)	0.838 (1)	0.85 (3)	0.85 (3)	0.997 (7)
O6—H6A	0.84 (2)	0.987 (5)	0.964 (1)	0.875 (1)	0.864 (1)	0.83 (3)	0.86 (3)	0.981 (6)
O6—H6B	0.83 (3)	0.988 (5)	0.906 (1)	0.897 (1)	0.886 (1)	0.84 (3)	0.85 (2)	0.985 (6)
O9—H9A	0.83 (2)	0.977 (5)	0.864 (1)	0.871 (1)	0.881 (2)	0.87 (3)	0.86 (2)	0.979 (5)
O9—H9B	0.84 (2)	0.984 (4)	0.884 (1)	0.901 (1)	0.964 (1)	0.87 (2)	0.87 (3)	0.966 (6)
O10—H10A	0.84 (4)	0.954 (5)	0.972 (1)	0.911 (1)	0.887 (1)	0.82 (2)	0.87 (2)	0.977 (8)
O10—H10B	0.84 (3)	0.972 (5)	0.855 (1)	0.821 (1)	0.913 (1)	0.84 (2)	0.85 (2)	0.978 (6)
O11—H11A	0.84 (3)	1.002 (5)	0.822 (1)	0.884 (1)	0.808 (1)	0.83 (3)	0.86 (2)	0.966 (6)
O11—H11B	0.83 (3)	0.965 (5)	0.906 (1)	0.859 (1)	0.900 (1)	0.84 (2)	0.84 (2)	0.966 (6)
Average O—H	0.84	0.975	0.897	0.874	0.882	0.85	0.85	0.977

(*a*) Elayaraja *et al.* (2007); (*b*) Howard *et al.* (2016); (*c*) Tepavitcharova *et al.* (2012); (*d*) Balamurugan *et al.* (2011); (*e*) Oguey *et al.* (2013*c*); (*f*) this work.

where the glycine zwitterion lies on a mirror plane, are values of 180° realized (Fleck & Bohatý, 2005). In α-glycine, the equivalent torsion angles are -19.60 (3) and 161.28 (2)°.

In respect of the heavy atoms, agreement in the interatomic distances and angles between the single-crystal X-ray and single-crystal neutron refinements (Table 1) is excellent, with some differences emerging in respect of the room-temperature refinement by Balamurugan *et al.* (2011). However, the neutron data provide a substantial improvement in accuracy with respect to the X-ray data in the hydrogen atom’s fractional coordinates and U_{ij} parameters. This is not surprising since neutrons are sensitive to the nuclear positions and X-rays to the electron density; in the covalent X—H bond the centroid of the H-atom’s electron-density distribution is displaced towards the heavy atom by 0.1 Å, yielding X—H distances from 10–15% shorter than the true internuclear separation (Coppens, 1997). Table 2 compares X—H bond lengths from a range of Gly·M(II)$SO_4\cdot 5H_2O$ crystals obtained by single-crystal X-ray diffraction and by neutron powder diffraction. In the work of Elayaraja *et al.* (2007), methyl

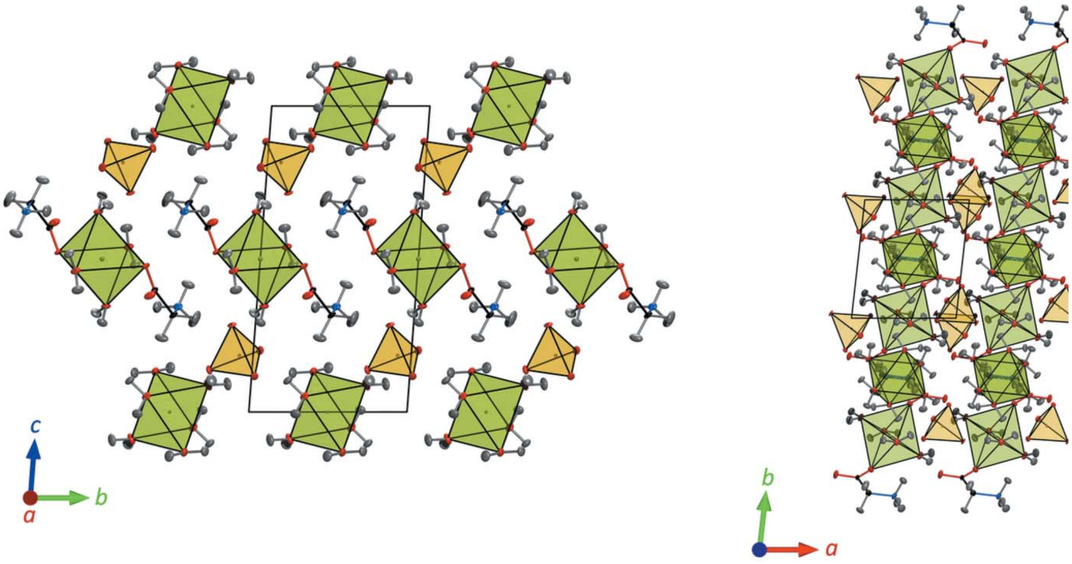

Figure 4
Packing of polyhedra in the structure of Glyc·$ZnSO_4\cdot 5H_2O$ viewed along *a* (left) and along *c* (right). ZnO_6 octahedra are green, SO_4 tetrahedra are yellow.

Table 3
Hydrogen-bond geometry (Å, °).

D—H···*A*	*D*—H	H···*A*	*D*···*A*	*D*—H···*A*
O5—H5*A*···O4$^{\mathrm{i}}$	0.973 (7)	1.793 (7)	2.755 (4)	169.0 (7)
O5—H5*B*···O8$^{\mathrm{ii}}$	0.997 (7)	1.656 (8)	2.642 (4)	168.9 (6)
O6—H6*A*···O3$^{\mathrm{iii}}$	0.981 (6)	1.722 (6)	2.696 (3)	170.8 (5)
O6—H6*B*···O4$^{\mathrm{iv}}$	0.985 (6)	1.751 (5)	2.729 (3)	171.8 (7)
O9—H9*A*···O1$^{\mathrm{iv}}$	0.979 (5)	1.732 (5)	2.707 (3)	173.8 (6)
O9—H9*B*···O2	0.966 (6)	1.895 (6)	2.811 (3)	157.2 (6)
O10—H10*A*···O3$^{\mathrm{iii}}$	0.977 (8)	1.740 (8)	2.713 (4)	173.0 (7)
O10—H10*B*···O2$^{\mathrm{v}}$	0.979 (6)	1.811 (7)	2.745 (4)	158.5 (7)
O11—H11*A*···O2$^{\mathrm{vi}}$	0.966 (6)	1.772 (6)	2.726 (3)	168.6 (6)
O11—H11*B*···O1	0.966 (6)	1.824 (6)	2.750 (3)	159.5 (7)
C2—H2*A*···O2$^{\mathrm{vi}}$	1.085 (6)	2.682 (9)	3.351 (4)	119.4 (6)
C2—H2*A*···O5$^{\mathrm{vii}}$	1.085 (6)	2.716 (8)	3.489 (3)	127.9 (6)
C2—H2*B*···O10	1.091 (7)	2.579 (8)	3.649 (4)	166.7 (7)
N1—H1*N*···O7$^{\mathrm{vii}}$	1.033 (7)	1.853 (7)	2.848 (3)	160.8 (7)
N1—H2*N*···O4	1.027 (8)	1.961 (7)	2.877 (3)	147.0 (7)
N1—H3*N*···O6	1.022 (6)	2.216 (7)	3.066 (3)	139.5 (5)

Symmetry codes: (i) $-x, -y+1, -z+1$; (ii) $x-1, y, z$; (iii) $x+1, y-1, z$; (iv) $x, y-1, z$; (v) $-x+1, -y+1, -z$; (vi) $x+1, y, z$; (vii) $-x+1, -y+1, -z+1$.

hydrogens were positioned geometrically and allowed to ride with $U_{\rm iso}$(H) = 1.2$U_{\rm eq}$(C); water hydrogen atoms were refined with restraints; the N—H bond lengths were all restrained to be equal. Balamurugan *et al.* (2011) placed the majority of their hydrogen atoms geometrically, although failed to identify the third amine hydrogen atom; water and the two amine H atoms were refined isotropically whereas the two methyl hydrogen atoms were riding on the C atom. Tepavitcharova *et al.* (2012) placed the hydrogen atoms in Gly·ZnSO$_4$·5H$_2$O geometrically and treated all of them as riding on their associated heavy atom during refinement. Oguey *et al.* (2013*c*) allowed all water hydrogen atoms to refine isotropically but fixed the methyl and amine hydrogens to ride on C and N, respectively. The coordinates of hydrogen atoms in this work were unrestrained and allowed to refine anisotropically.

Our values for the N—H and C—H bond lengths are in excellent agreement with other single-crystal neutron diffraction work, as noted in the preceding paragraph. Our values for the O—H bond lengths also agree well with those found in similar environments in hydrated *M*(II) coordination compounds, such as MgSO$_4$·11H$_2$O and MgCrO$_4$·11H$_2$O where the average O–H = 0.974 Å (Fortes *et al.*, 2013), MgSeO$_4$·9H$_2$O, O—H$_{\rm av}$ = 0.972 Å (Fortes *et al.*, 2015), and MgSeO$_4$·7H$_2$O, O—H$_{\rm av}$ = 0.974 Å (Fortes & Gutmann, 2014).

3. Supramolecular features

The overall three-dimensional framework is completed by a variety of hydrogen bonds with a range of strengths (Table 3). Fig. 4 shows the spatial relationship of the main structural elements. The majority of the hydrogen bonds are O—H···O contacts of medium strength (1.66 < H···O < 1.90 Å) and high linearity (∠ O—H···O > 157°), characteristic of two-centred interactions. As expected, the N—H···O hydrogen bonds are weaker (*i.e.*, longer, 1.85 < H···O < 2.22 Å) and more strained (∠ N—H···O between approx. 140–160°). The methyl groups appear to participate in weak C—H···O hydrogen bonds (*cf.*, Steiner & Desiraju, 1998). One C—H···O bond is evidently a two-centred interaction, being the shortest and most of linear contact of this kind, with H···O = 2.58 (1) Å and ∠ C—H···O = 167 (1)°. The other, involving C—H2*A*, is clearly a two-centred interaction (*i.e.*, a bifurcated hydrogen bond) with 'arms' of roughly equal length, H···O ≃ 2.7 Å and C—H···O angles of 119 and 128° involving O2 and O5, respectively.

3.1. Glycine dimers

A hitherto unrecognized aspect of the supramolecular structure of Glyc·*M*(II)SO$_4$·5H$_2$O compounds is the presence of glycine dimers (Fig. 5). These occur as closed cyclic structures formed by N—H···O hydrogen bonds between the amine group of one glycine zwitterion and the Zn-coordinating carboxylate oxygen (O7) of another zwitterion, related to the first by an inversion centre. A similar cyclic dimer occurs in the structure of α-glycine. A direct comparison between the dimers in Glyc·ZnSO$_4$·5H$_2$O and in α-glycine is shown in Fig. 6; clearly, the main difference between these two dimers is the orientation of the carboxylate group, which is presumably due to the influence of a divalent metal being coordinated by

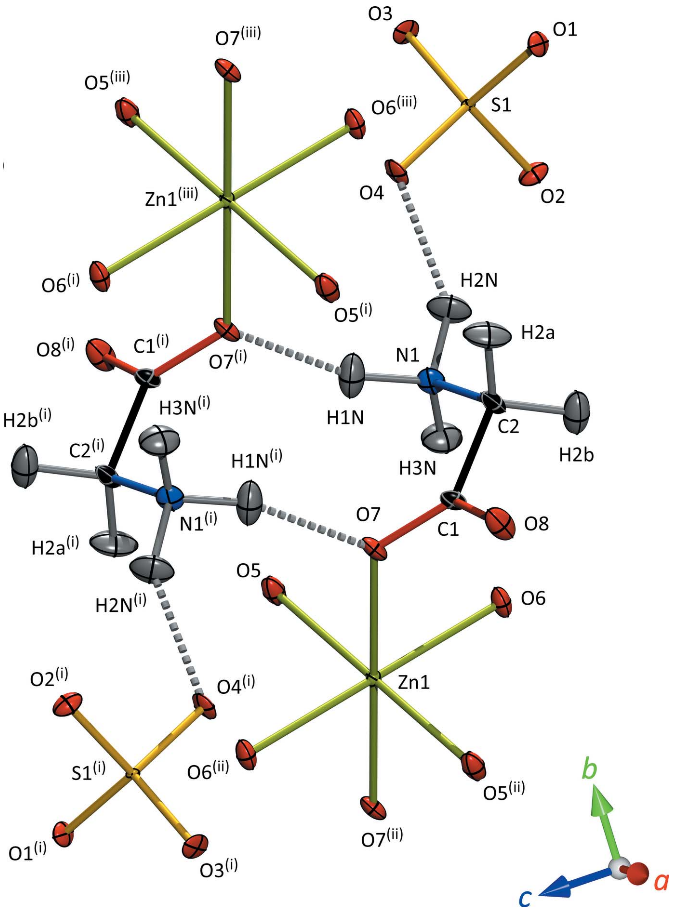

Figure 5
Connectivity between adjacent Zn1 octahedra is *via* a closed cyclic glycine dimer. As before, displacement ellipsoids are drawn at the 50% probability level for H and 90% for all other atoms. Dashed lines indicate N—H···O hydrogen bonds. [Symmetry codes: (i) $1-x, 1-y, 1-z$; (ii) $1-x, -y, 1-z$; (iii) $x, 1+y, z$.]

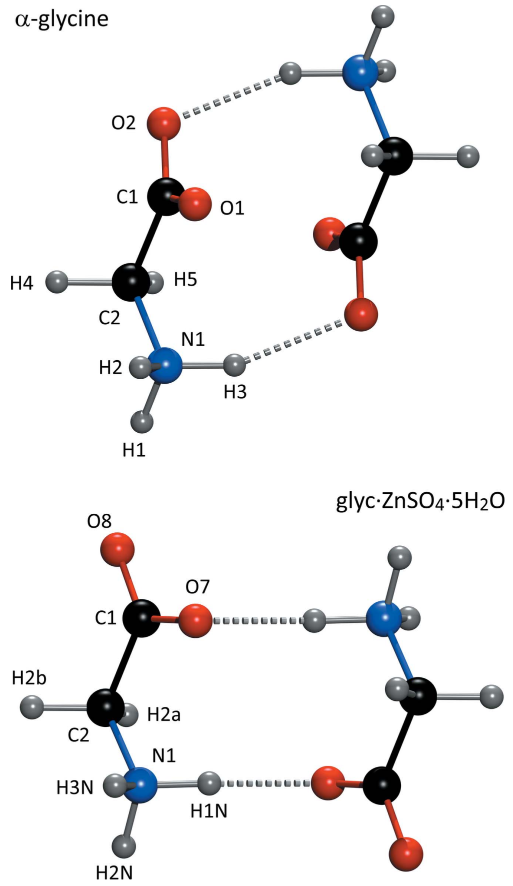

Figure 6
Comparison of the closed cyclic dimers involving zwitterionic glycine that occur in the crystal structures of α-glycine (top) and in Glyc·$ZnSO_4$·$5H_2O$ (bottom).

the O7 carboxylate oxygen. Experimental studies of aqueous solutions indicate that only glycine monomers exist in the liquid phase (Huang *et al.*, 2008). However, there has been widespread disagreement on this matter from computational studies, which indicate either that there are no dimers (Hamad & Catlow, 2011), substantial quantities of closed zwitterionic dimers (Friant-Michel & Ruiz-López, 2010), or a small fraction of open dimers (Yani *et al.*, 2012) present in saturated solutions. The presence or absence of glycine polymerization in coordination compounds such as these may be useful in understanding the association of glycine in saturated aqueous solutions during nucleation and the role of solvated metal ions in polymerizing amino acids in Earth's Hadean oceans (Kitadai *et al.*, 2011, 2016) or in extraterrestrial oceans elsewhere in our solar system (Kimura & Kitadai, 2015).

4. Database survey

A search of the Cambridge Structural Database (Groom *et al.*, 2016) identified the following directly relevant entries:

Glyc·*M*(II)SO_4 pentahydrates: 672589 (Mg); 857075 (Mg); 1451396 (Mg); 296329 (Co); 857073 (Co); 806684 (Zn); 857076 (Zn); 936400 (Zn).

Table 4
Raman vibrational frequencies and mode assignments of α-glycine (*cf.*, Stenbäck, 1976: Rosado *et al.*, 1998: Yang *et al.*, 2008), Glyc·$MgSO_4$·$5H_2O$ (Howard *et al.*, 2016) and the title compound.

Meaning of symbols: ν = stretch; δ = deformation; ρ = rock; ω = wag; Γ = twist; (*A*) = asymmetric; (*S*) = symmetric.

	α-Glycine[a]	Glyc·$MgSO_4$·$5H_2O$[a]	Glyc·$ZnSO_4$·$5H_2O$
Vibrational mode	180 s, 18 mW	1400 s, 18 mW	540 s, 18 mW
δ M^{2+}—O (?)	–	208	203
	–	236	220
δ CCN^+	356	361	382
ρ COO^-			
$\delta(S)$ SO_4^{2-}	–	453	451
ρ COO^-	497	522	527
ω COO^-	601	597	582
			599
$\delta(A)$ SO_4^{2-}		623	626
		645	644
δ COO^-	696	–	–
unknown	–	794	–
ν C—C^+	893	890	890
ν C—N		905	906
ν C—O			
ρ CH_2	922	–	–
$\nu(S)$ SO_4^{2-}	–	983.8	983.2
ν C—N	1036	1020	1021
$\nu(A)$ SO_4^{2-}	–	1077	1078
		1100	1101
ρ NH^{3+}	1108	1139	1141
	1140		
ω CH_2	1325	1305	1306
Γ CH_2		1328	1327
$\nu(S)$ COO^-	1410	1395	1391
$\delta(S)$ CH_2	1441	1434	1433
	1457		
$\delta(A)$ NH^{3+}	1502		
$\delta(S)$ NH^{3+}	1516	1488	1488
	1569		
ν C—C^+	1634	1597	1590
ω CH_2			
$\nu(A)$ COO^-	1670	1631	1614
$\nu(S)$ CH_2	2972	2997	2996
$\nu(A)$ CH_2	3009	3038	3037
$\nu(S)$ NH^{3+}	3143	–	–
$\nu(S)$ H_2O	–	3248	3204
			3233
$\nu(A)$ H_2O	–	3384	3331
			3405

[a] Howard *et al.* (2016).

Glyc·*M*(II)SO_4 trihydrates: 989590 (Mg); 1451397 (Mg); 857074 (Co); 936396 (Fe); 243588 (Zn, orthorhombic); 936394 (Zn, monoclinic).

Glyc·*M*(II)SO_4 hexahydrates: 1285639 (Ni).

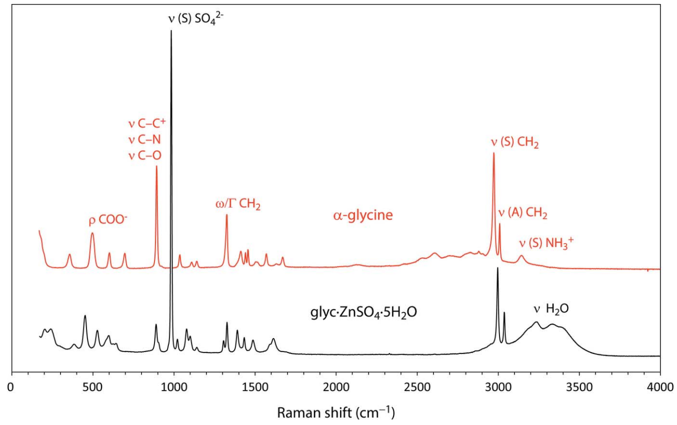

Figure 7
Raman spectra of *α*-glycine (top) and Glyc·$ZnSO_4$·$5H_2O$ (bottom). Selected vibrational modes are labelled and a complete quantitative listing is given in Table 4.

5. Vibrational spectroscopy

Laser-stimulated Raman spectra were measured using a portable B&WTek *i*-Raman Plus spectrometer equipped with a 532 nm laser (P_{max} = 37 mW at the probe tip) that records spectra over the range 171–4002 cm^{-1} with an optimal resolution of 3 cm^{-1}. Measurements were carried out on powdered specimens of *α*-glycine and Glyc·$ZnSO_4$·$5H_2O$. Samples were measured in thin-walled glass vials using the BC100 fibre-optic coupled Raman probe; the total integration time and laser power for each sample is provided with the tabulated results (see supplementary material).

The Raman spectrum of Glyc·$ZnSO_4$·$5H_2O$ (Fig. 6) is virtually identical with that of Glyc·$MgSO_4$·$5H_2O$ reported in Howard *et al.* (2016) and is in excellent agreement with the spectrum shown in Tepavitcharova *et al.* (2012). Numerical data of the Raman spectrum are provided as an electronic supplement; peak positions and vibrational mode assignments are given in Table 4. The main differences between the two divalent-metal-substituted compounds include the blue-shifting of octahedral deformation modes and blue-shifting of both symmetric and asymmetric COO^- stretching modes. A large blue-shift of *ν*(*A*) and *ν*(*S*) COO^- occurs when glycine coordinates to Mg^{2+} and the shift increases when glycine coordinates to Zn^{2+}. Raman spectra of *α*-glycine and Glyc·$ZnSO_4$·$5H_2O$ are shown in Fig. 7.

6. Synthesis and crystallization

Glyc·$ZnSO_4$·$5H_2O$ was crystallized by evaporation at room temperature of an equimolar aqueous solution of *α*-glycine (Alfa Aesar A13816) and $ZnSO_4$·$7H_2O$ (Sigma Aldrich Z4750) in deionized water (Alfa Aesar 36645). Unlike the $MgSO_4$-bearing analogue, Glyc·$ZnSO_4$·$5H_2O$ forms large well-faceted crystals that are both amenable to morphological study and suitably large for single-crystal neutron diffraction analysis. Fig. 1 shows photographs of a representative crystal viewed along its *a* axis and series of drawings with indexed crystal faces.

7. Data collection and refinement

Crystal data, data collection and structure refinement details are summarized in Table 5. Data were collected from a pair of single crystals at a series of four discrete rotational positions about the vertical axis, each frame being counted for 5 h, equivalent to 800 µAhr of ISIS proton beam current per frame. The structure of Glyc(d_5)·$MgSO_4$·$5D_2O$ at 10 K reported by Howard *et al.* (2016) was used as a starting point for the refinement. A total of eleven peaks, with the largest $\sigma(F_{obs}–F_{calc})$ values were omitted from the refinement; such outliers are fairly common in SXD measurement when peaks occur close to the edges of detectors. A mild restraint on the U_{ij} parameters of the sulfur atom was imposed (*SHELX* ISOR command) in order to avoid a slightly non-positive-definite displacement ellipsoid. Since sulfur has the smallest neutron scattering cross section of any atom in the structure, and since it is both comparatively heavy and the temperature is very low, it is not surprising that – within errors – the effective U_{iso} parameter should refine to a small negative value.

Table 5
Experimental details.

Crystal data	
Chemical formula	$[Zn(H_2O)_6][Zn(C_2H_5NO_2)_2(H_2O)_4](SO_4)_2$
M_r	653.20
Crystal system, space group	Triclinic, $P\overline{1}$
Temperature (K)	10
a, *b*, *c* (Å)	5.9601 (15), 6.7670 (17), 13.112 (4)
α, *β*, *γ* (°)	84.955 (18), 83.25 (2), 83.042 (19)
V ($Å^3$)	519.8 (2)
Z	1
Radiation type	Neutron, λ = 0.48-7.0 Å
µ (mm^{-1})	5.02 + 0.0182 * λ
Crystal size (mm)	4 × 2.5 × 1
Data collection	
Diffractometer	SXD
Absorption correction	Numerical. The linear absorption coefficient is wavelength dependent and is calculated as: *µ* = 5.0165 + 0.0182 * λ [cm^{-1}] as determined by Gaussian integration in *SXD2001* (Gutmann, 2005)
No. of measured, independent and observed [$I > 2\sigma(I)$] reflections	8296, 8296, 8296
R_{int}	0.089
Refinement	
$R[F^2 > 2\sigma(F^2)]$, $wR(F^2)$, *S*	0.089, 0.246, 1.09
No. of reflections	8296
No. of parameters	291
No. of restraints	12
H-atom treatment	All H-atom parameters refined
$\Delta\rho_{max}$, $\Delta\rho_{min}$ (e $Å^{-3}$)	3.20, −3.47

Computer programs: *SXD2001* (Gutmann, 2005), *SHELXT2014* (Sheldrick, 2015*a*; Gruene *et al.*, 2014), *SHELXL2014* (Sheldrick, 2015*b*; Gruene *et al.*, 2014), *DIAMOND* (Putz & Brandenburg, 2006) and *publCIF* (Westrip, 2010).

Acknowledgements

The authors thank the STFC ISIS facility for beam-time access. IGW acknowledges a grant from STFC, No. ST/K000934/1; CMH is similarly supported by a postgraduate studentship from STFC.

References

Alymkulova, K. & Salyeva, N. V. (1987). *Koordinatsionnye Soedinenija Metallov s Bioligandami, Institut Neorganicheskoj i Fizicheskoj Khimii* pp. 77–79. Kyrgyz SSR Ilimder Akademijasy. (In Russian).

Balakrishnan, T. & Ramamurthy, K. (2007). *Spectrochim. Acta A*, **68**, 360–363.

Balamurugan, M. S., Subramanian, P. & Rao, P. S. (2011). Private communication (Deposition number CCDC 8606684). CCDC, Cambridge, England. DOI: 10.5517/ccw2f2f.

Coppens, P. (1997). *X-ray Charge Density and Chemical Bonding*. Oxford University Press, Oxford, England.

Elayaraja, K., Parthiban, S. P., Ramalingom, S., Bocelli, G. & Kalkura, S. N. (2007). *Acta Cryst.* E**63**, m2901–m2902.

El-Fadl, A. A. & Abdulwahab, A. M. (2010). *Physica B*, **405**, 3421–3426.

Fleck, M. & Bohatý, L. (2004). *Acta Cryst.* C**60**, m291–m295.

Fleck, M. & Bohatý, L. (2005). *Acta Cryst.* C**61**, m412–m416.

Fleck, M. & Bohatý, L. (2006). *Acta Cryst.* C**62**, m22–m26.

Fortes, A. D., Alfè, D., Hernández, E. R. & Gutmann, M. J. (2015). *Acta Cryst.* B**71**, 313–327.

Fortes, A. D. & Gutmann, M. J. (2014). *Acta Cryst.* E**70**, 134–137.

Fortes, A. D., Wood, I. G. & Gutmann, M. J. (2013). *Acta Cryst.* C**69**, 324–329.

Friant-Michel, P. & Ruiz-López, M. F. (2010). *ChemPhysChem*, **11**, 3499–3504.

Groom, C. R., Bruno, I. J., Lightfoot, M. P. & Ward, S. C. (2016). *Acta Cryst.* B**72**, 171–179.

Gruene, T., Hahn, H. W., Luebben, A. V., Meilleur, F. & Sheldrick, G. M. (2014). *J. Appl. Cryst.* **47**, 462–466.

Gutmann, M. J. (2005). *SXD2001*. ISIS Facility, Rutherford Appleton Laboratory, Oxfordshire, England.

Hamad, S. & Catlow, C. R. A. (2011). *CrystEngComm*, **13**, 4391–4399.

Howard, C., Wood, I. G., Knight, K. S. & Fortes, A. D. (2016). *Acta Cryst.* C**72**, 203–216.

Huang, J., Stringfellow, T. C. & Yu, L. (2008). *J. Am. Chem. Soc.* **130**, 13973–13980.

Jönsson, P.-G. & Kvick, Å. (1972). *Acta Cryst.* B**28**, 1827–1833.

Kaminsky, W. (2005). *J. Appl. Cryst.* **38**, 566–567.

Kaminsky, W. (2007). *J. Appl. Cryst.* **40**, 382–385.

Kimura, J. & Kitadai, N. (2015). *Astrobiology*, **15**, 430–441.

Kitadai, N. (2016). *Orig. Life Evol. Biosph.* **10**, 1007s11084-016-9510-5.

Kitadai, N., Yokoyama, T. & Nakashima, S. (2011). *Geochim. Cosmochim. Acta*, **75**, 6285–6299.

Lindqvist, I. & Rosenstein, R. (1960). *Acta Chem. Scand.* **14**, 1228–1229.

Moldobaev, S. & Nogoev, K. (1970). *Materialy Nauchnoi Konferentsii Posvyashchennoy 100-letiyu Periodicheskogo Zakona D. I. Mendeleeva*, C-29. (In Russian).

Moldobaev, S., Nogoev, K. & Ismailov, T. (1970). *Materialy Nauchnoi Konferentsii Posvyashchennoy 100-letiyu Periodicheskogo Zakona D. I. Mendeleeva*, C-120. (In Russian).

Oguey, S., Jacquier, Y., Neels, A. & Stoeckli-Evans, H. (2013*a*). Private communication (deposit number CCDC 936393). CCDC, Cambridge, England. DOI: 10.5517/cc10fd72

Oguey, S., Jacquier, Y., Neels, A. & Stoeckli-Evans, H. (2013*b*). Private communication (deposit number CCDC 936394. CCDC, Union Road, Cambridge, England. DOI: 10.5517/cc10fd83

Oguey, S., Jacquier, Y., Neels, A. & Stoeckli-Evans, H. (2013*c*). Private communication (deposit number CCDC 936400). CCDC, Cambridge, England. DOI: 10.5517/cc10fdg9

Oguey, S., Jacquier, Y., Sereda, O., Neels, A. & Stoeckli-Evans, H. (2014). Private communication (deposit number CCDC 989590). CCDC, Cambridge, England. DOI: 10.5517/cc126r89

Power, L. F., Turner, K. E. & Moore, F. H. (1976). *Acta Cryst.* B**32**, 11–16.

Putz, H. & Brandenburg, K. (2006). *DIAMOND*. Crystal Impact GbR, Bonn, Germany.

Robinson, K., Gibbs, G. V. & Ribbe, P. H. (1971). *Science*, **172**, 567–570.

Rosado, M. T., Duarte, M. L. T. S. & Fausto, R. (1998). *Vib. Spectrosc.* **16**, 35–54.

Sheldrick, G. M. (2015*a*). *Acta Cryst.* A**71**, 3–8.

Sheldrick, G. M. (2015*b*). *Acta Cryst.* C**71**, 3–8.

Steiner, T. & Desiraju, G. R. (1998). *Chem. Commun.* pp. 891–892.

Stenbäck, H. (1976). *J. Raman Spectrosc.* **5**, 49–55.

Tepavitcharova, S., Rabadjieva, D., Havlíček, D., Němec, I., Vojtíšek, P., Plocek, J. & Koleva, Z. (2012). *J. Mol. Struct.* **1018**, 113–121.

Thilagavathi, R., Selvarajan, P. & Kumari, V. V. (2012). *Int. J. Adv. Sci. Tech. Res*, **2**, 164–183.

Westrip, S. P. (2010). *J. Appl. Cryst.* **43**, 920–925.

Yang, X., Lu, J., Wang, X. & Ching, C. B. (2008). *J. Raman Spectrosc.* **39**, 1433–1439.

Yani, Y., Chow, P. S. & Tan, R. B. H. (2012). *Cryst. Growth Des.* **12**, 4771–4778.

supporting information

Acta Cryst. (2016). E**72**, 1438-1445 [doi:10.1107/S2056989016014304]

Glycine zinc sulfate pentahydrate: redetermination at 10 K from time-of-flight neutron Laue diffraction

A. Dominic Fortes, Christopher M. Howard, Ian G. Wood and Matthias J. Gutmann

Computing details

Data collection: *SXD2001* (Gutmann, 2005); cell refinement: *SXD2001* (Gutmann, 2005); data reduction: *SXD2001* (Gutmann, 2005); program(s) used to solve structure: SHELXT2014 (Sheldrick, 2015a; Gruene *et al.*, 2014); program(s) used to refine structure: *SHELXL2014* (Sheldrick, 2015b; Gruene *et al.*, 2014); molecular graphics: *DIAMOND* (Putz & Brandenburg, 2006); software used to prepare material for publication: *publCIF* (Westrip, 2010).

Hexaaquazinc(II) tetraaquadiglycinezinc(II) bis(sulfate)

Crystal data

$[Zn(H_2O)_6][Zn(C_2H_5NO_2)_2(H_2O)_4](SO_4)_2$
$M_r = 653.20$
Triclinic, $P\bar{1}$
$a = 5.9601\ (15)$ Å
$b = 6.7670\ (17)$ Å
$c = 13.112\ (4)$ Å
$\alpha = 84.955\ (18)°$
$\beta = 83.25\ (2)°$
$\gamma = 83.042\ (19)°$
$V = 519.8\ (2)$ Å^3

$Z = 1$
$F(000) = 336$
$D_x = 2.086$ Mg m^{-3}
Neutron radiation, $\lambda = 0.48\text{-}7.0$ Å
Cell parameters from 550 reflections
$\mu = 5.02 + 0.0182 * \lambda$ mm^{-1}
$T = 10$ K
Tabular, colourless
4 × 2.5 × 1 mm

Data collection

SXD
diffractometer
Radiation source: ISIS neutron spallation source
time–of–flight LAUE diffraction scans
Absorption correction: numerical
The linear absorption coefficient is wavelength dependent and is calculated as: $\mu = 5.0165 + 0.0182 * \lambda$ [cm^{-1}] as determined by Gaussian integration in *SXD2001* (Gutmann, 2005)

8296 measured reflections
8296 independent reflections
8296 reflections with $I > 2\sigma(I)$
$R_{int} = 0.089$
$\theta_{max} = 87.4°$, $\theta_{min} = 8.2°$
$h = -15 \rightarrow 15$
$k = -18 \rightarrow 16$
$l = -28 \rightarrow 29$

Refinement

Refinement on F^2
Least-squares matrix: full
$R[F^2 > 2\sigma(F^2)] = 0.089$
$wR(F^2) = 0.246$
$S = 1.09$
8296 reflections
291 parameters
12 restraints
Hydrogen site location: difference Fourier map

All H-atom parameters refined
$w = 1/[\sigma^2(F_o^2) + (0.1376P)^2 + 36.2519P]$
where $P = (F_o^2 + 2F_c^2)/3$
$(\Delta/\sigma)_{max} < 0.001$
$\Delta\rho_{max} = 3.20$ e Å^{-3}
$\Delta\rho_{min} = -3.47$ e Å^{-3}
Extinction correction: SHELXL,
$Fc^* = kFc[1+0.001xFc^2\lambda^3/\sin(2\theta)]^{-1/4}$
Extinction coefficient: 0.0386 (18)

Special details

Experimental. For peak integration a local UB matrix refined for each frame, using approximately 50 reflections from each of the 11 detectors. Hence _cell_measurement_reflns_used 550 For final cell dimensions a weighted average of all local cells was calculated Because of the nature of the experiment, it is not possible to give values of theta_min and theta_max for the cell determination. The same applies for the wavelength used for the experiment. The range of wavelengths used was 0.48–7.0 Angstroms, BUT the bulk of the diffraction information is obtained from wavelengths in the range 0.7–2.5 Angstroms. The data collection procedures on the SXD instrument used for the single-crystal neutron data collection are most recently summarized in the Appendix to the following paper Wilson, C.C. (1997). J. Mol. Struct. 405, 207–217

Geometry. All esds (except the esd in the dihedral angle between two l.s. planes) are estimated using the full covariance matrix. The cell esds are taken into account individually in the estimation of esds in distances, angles and torsion angles; correlations between esds in cell parameters are only used when they are defined by crystal symmetry. An approximate (isotropic) treatment of cell esds is used for estimating esds involving l.s. planes.

Refinement. The variable wavelength nature of the data collection procedure means that sensible values of _diffrn_reflns_theta_min & _diffrn_reflns_theta_max cannot be given instead the following limits are given _diffrn_reflns_sin(theta)/lambda_min 0.06 _diffrn_reflns_sin(theta)/lambda_max 1.38 _refine_diff_density_max/min is given in Fermi per angstrom cubed not electons per angstrom cubed. Another way to consider the _refine_diff_density_ is as a percentage of the scattering density of a given atom: _refine_diff_density_max = 5.7 % of hydrogen _refine_diff_density_min = -6.1 % of hydrogen Refinement of F^2 against ALL reflections. The weighted R-factor wR and goodness of fit S are based on F^2, conventional R-factors R are based on F, with F set to zero for negative F^2. The threshold expression of $F^2 > \sigma(F^2)$ is used only for calculating R-factors(gt) *etc*. and is not relevant to the choice of reflections for refinement. R-factors based on F^2 are statistically about twice as large as those based on F, and R- factors based on ALL data will be even larger.

Fractional atomic coordinates and isotropic or equivalent isotropic displacement parameters (Å²)

	x	y	z	U_{iso}*/U_{eq}
S1	0.0141 (6)	0.9128 (6)	0.1847 (4)	0.0008 (6)
O1	0.1809 (4)	1.0196 (3)	0.1159 (2)	0.0036 (4)
O2	−0.0249 (4)	0.7303 (3)	0.1375 (2)	0.0037 (4)
O3	−0.2027 (4)	1.0416 (3)	0.2010 (2)	0.0040 (4)
O4	0.1050 (4)	0.8522 (4)	0.2845 (2)	0.0038 (3)
Zn1	0.5000	0.0000	0.5000	0.0017 (4)
O5	0.1954 (4)	0.1618 (4)	0.5392 (2)	0.0049 (4)
H5A	0.0913 (11)	0.1389 (11)	0.6009 (6)	0.0198 (11)
H5B	0.0998 (10)	0.2109 (9)	0.4826 (6)	0.0170 (10)
O6	0.4360 (4)	0.0464 (4)	0.3456 (2)	0.0043 (4)
H6A	0.5654 (10)	0.0305 (9)	0.2922 (5)	0.0162 (10)
H6B	0.3082 (10)	−0.0116 (10)	0.3229 (6)	0.0179 (11)
O7	0.6512 (4)	0.2793 (4)	0.4768 (2)	0.0037 (3)
O8	0.9812 (4)	0.3195 (4)	0.3809 (2)	0.0060 (4)
N1	0.3991 (2)	0.5025 (2)	0.34432 (14)	0.0044 (2)
H1N	0.3634 (11)	0.5559 (12)	0.4165 (6)	0.0218 (13)
H2N	0.3159 (12)	0.6073 (10)	0.2963 (7)	0.0212 (12)
H3N	0.3294 (11)	0.3719 (9)	0.3435 (6)	0.0199 (12)
C1	0.7711 (3)	0.3465 (3)	0.39746 (19)	0.0029 (3)
C2	0.6484 (3)	0.4781 (3)	0.3163 (2)	0.0041 (3)
H2A	0.7111 (11)	0.6233 (9)	0.3086 (7)	0.0220 (13)
H2B	0.6871 (11)	0.4134 (12)	0.2420 (6)	0.0222 (13)
Zn2	0.5000	0.5000	0.0000	0.0008 (3)

O9	0.2958 (4)	0.3897 (3)	0.1320 (2)	0.0045 (4)
H9A	0.2434 (11)	0.2593 (8)	0.1279 (6)	0.0175 (11)
H9B	0.1606 (10)	0.4824 (9)	0.1443 (6)	0.0190 (11)
O10	0.7911 (4)	0.3443 (4)	0.0509 (2)	0.0048 (4)
H10A	0.7828 (12)	0.2322 (9)	0.1030 (6)	0.0180 (10)
H10B	0.8989 (11)	0.2959 (10)	−0.0061 (6)	0.0197 (11)
O11	0.5434 (4)	0.7298 (4)	0.0881 (2)	0.0054 (4)
H11A	0.6938 (9)	0.7484 (9)	0.1036 (6)	0.0182 (11)
H11B	0.4422 (10)	0.8523 (8)	0.0915 (7)	0.0200 (12)

Atomic displacement parameters (Å^2)

	U^{11}	U^{22}	U^{33}	U^{12}	U^{13}	U^{23}
S1	0.0006 (10)	0.0009 (11)	0.0010 (18)	0.0001 (8)	−0.0003 (9)	0.0000 (11)
O1	0.0027 (6)	0.0037 (7)	0.0038 (10)	−0.0006 (5)	0.0016 (5)	0.0001 (7)
O2	0.0029 (6)	0.0028 (6)	0.0058 (11)	−0.0007 (5)	−0.0007 (6)	−0.0012 (7)
O3	0.0017 (6)	0.0040 (7)	0.0053 (11)	0.0018 (5)	0.0010 (6)	0.0000 (7)
O4	0.0039 (6)	0.0054 (7)	0.0018 (10)	0.0001 (5)	−0.0015 (6)	0.0011 (7)
Zn1	0.0015 (4)	0.0017 (4)	0.0017 (5)	−0.0001 (3)	−0.0001 (3)	0.0000 (3)
O5	0.0036 (7)	0.0071 (8)	0.0032 (11)	0.0014 (5)	−0.0002 (6)	0.0011 (7)
H5A	0.015 (2)	0.028 (3)	0.014 (3)	−0.0027 (18)	0.0046 (18)	0.002 (2)
H5B	0.015 (2)	0.019 (2)	0.016 (3)	0.0017 (15)	−0.0065 (17)	0.004 (2)
O6	0.0041 (7)	0.0064 (7)	0.0021 (11)	−0.0005 (5)	−0.0004 (6)	0.0002 (7)
H6A	0.0142 (18)	0.021 (2)	0.013 (3)	−0.0020 (15)	0.0034 (16)	−0.005 (2)
H6B	0.017 (2)	0.023 (2)	0.017 (3)	−0.0076 (17)	−0.0052 (18)	−0.005 (2)
O7	0.0042 (6)	0.0041 (7)	0.0026 (10)	−0.0011 (5)	−0.0004 (6)	0.0014 (7)
O8	0.0028 (7)	0.0091 (9)	0.0050 (12)	0.0008 (5)	0.0001 (6)	0.0022 (8)
N1	0.0030 (4)	0.0057 (5)	0.0041 (7)	0.0012 (3)	−0.0013 (4)	0.0004 (5)
H1N	0.017 (2)	0.033 (3)	0.015 (3)	0.002 (2)	0.0004 (19)	−0.009 (3)
H2N	0.019 (2)	0.020 (2)	0.025 (4)	0.0015 (18)	−0.011 (2)	0.006 (2)
H3N	0.018 (2)	0.015 (2)	0.027 (4)	−0.0066 (16)	−0.001 (2)	0.001 (2)
C1	0.0020 (5)	0.0034 (6)	0.0032 (9)	0.0000 (4)	−0.0011 (5)	0.0007 (6)
C2	0.0042 (6)	0.0047 (6)	0.0030 (9)	−0.0002 (4)	−0.0004 (5)	0.0017 (6)
H2A	0.020 (2)	0.013 (2)	0.033 (4)	−0.0078 (17)	−0.005 (2)	0.007 (2)
H2B	0.018 (2)	0.035 (3)	0.013 (3)	0.007 (2)	−0.0031 (19)	−0.006 (3)
Zn2	0.0008 (4)	0.0008 (4)	0.0009 (5)	−0.0001 (3)	−0.0001 (3)	0.0001 (3)
O9	0.0045 (7)	0.0035 (7)	0.0050 (11)	−0.0005 (5)	0.0005 (6)	0.0004 (7)
H9A	0.021 (2)	0.0115 (17)	0.021 (3)	−0.0064 (15)	−0.001 (2)	−0.001 (2)
H9B	0.0135 (19)	0.016 (2)	0.024 (4)	0.0064 (14)	0.0009 (18)	−0.001 (2)
O10	0.0039 (7)	0.0047 (7)	0.0050 (11)	0.0019 (5)	−0.0012 (6)	0.0010 (7)
H10A	0.024 (3)	0.015 (2)	0.013 (3)	0.0011 (17)	0.0002 (19)	0.0054 (19)
H10B	0.020 (2)	0.020 (2)	0.016 (3)	0.0065 (17)	0.0040 (19)	−0.002 (2)
O11	0.0033 (6)	0.0048 (7)	0.0086 (12)	0.0002 (5)	−0.0015 (6)	−0.0033 (8)
H11A	0.0091 (16)	0.022 (2)	0.025 (3)	−0.0030 (15)	−0.0057 (17)	−0.004 (2)
H11B	0.017 (2)	0.0118 (18)	0.031 (4)	0.0059 (14)	−0.003 (2)	−0.006 (2)

Geometric parameters (Å, º)

S1—O3	1.473 (4)	N1—H1N	1.033 (7)
S1—O1	1.474 (5)	N1—C2	1.481 (2)
S1—O4	1.480 (6)	C1—C2	1.523 (4)
S1—O2	1.484 (4)	C2—H2A	1.085 (6)
Zn1—O5	2.039 (2)	C2—H2B	1.091 (7)
Zn1—O5^{i}	2.039 (2)	Zn2—O10	2.067 (3)
Zn1—O6	2.093 (3)	Zn2—O10^{ii}	2.067 (3)
Zn1—O6^{i}	2.094 (3)	Zn2—O11^{ii}	2.075 (2)
Zn1—O7^{i}	2.173 (2)	Zn2—O11	2.075 (2)
Zn1—O7	2.173 (2)	Zn2—O9	2.129 (3)
O5—H5A	0.973 (7)	Zn2—O9^{ii}	2.129 (3)
O5—H5B	0.997 (7)	O9—H9B	0.966 (6)
O6—H6A	0.981 (6)	O9—H9A	0.979 (5)
O6—H6B	0.985 (6)	O10—H10A	0.977 (8)
O7—C1	1.272 (4)	O10—H10B	0.979 (6)
O8—C1	1.240 (3)	O11—H11B	0.966 (6)
N1—H3N	1.022 (6)	O11—H11A	0.966 (6)
N1—H2N	1.027 (8)		

O3—S1—O1	110.2 (3)	O8—C1—O7	126.0 (3)
O3—S1—O4	110.1 (3)	O8—C1—C2	116.2 (2)
O1—S1—O4	109.5 (3)	O7—C1—C2	117.7 (2)
O3—S1—O2	109.3 (3)	H2A—C2—H2B	107.9 (7)
O1—S1—O2	109.3 (3)	H2A—C2—N1	109.5 (4)
O4—S1—O2	108.4 (3)	H2B—C2—N1	109.5 (4)
O5—Zn1—O5^{i}	180.0	H2A—C2—C1	108.5 (5)
O5—Zn1—O6	88.59 (11)	H2B—C2—C1	109.7 (4)
O5^{i}—Zn1—O6	91.41 (11)	O10—Zn2—O10^{ii}	180.0
O5—Zn1—O6^{i}	91.41 (11)	O10—Zn2—O11^{ii}	91.57 (10)
O5^{i}—Zn1—O6^{i}	88.59 (11)	O10^{ii}—Zn2—O11^{ii}	88.43 (10)
O6—Zn1—O6^{i}	180.0	O10—Zn2—O11	88.43 (10)
O5—Zn1—O7^{i}	92.01 (9)	O10^{ii}—Zn2—O11	91.57 (10)
O5^{i}—Zn1—O7^{i}	87.99 (9)	O11^{ii}—Zn2—O11	180.0
O6—Zn1—O7^{i}	93.38 (10)	O10—Zn2—O9	91.52 (11)
O6^{i}—Zn1—O7^{i}	86.62 (10)	O10^{ii}—Zn2—O9	88.48 (11)
O5—Zn1—O7	87.99 (9)	O11^{ii}—Zn2—O9	94.16 (10)
O5^{i}—Zn1—O7	92.01 (9)	O11—Zn2—O9	85.84 (10)
O6—Zn1—O7	86.62 (10)	O10—Zn2—O9^{ii}	88.48 (11)
O6^{i}—Zn1—O7	93.38 (10)	O10^{ii}—Zn2—O9^{ii}	91.52 (11)
O7^{i}—Zn1—O7	180.0	O11^{ii}—Zn2—O9^{ii}	85.84 (10)
H5A—O5—H5B	106.7 (6)	O11—Zn2—O9^{ii}	94.16 (10)
H6A—O6—H6B	108.1 (6)	O9—Zn2—O9^{ii}	180.00 (12)
C1—O7—Zn1	128.26 (18)	H9B—O9—H9A	106.2 (6)
H3N—N1—H2N	107.6 (6)	H10A—O10—H10B	106.1 (6)

H3N—N1—H1N	109.8 (7)	H11B—O11—H11A	111.4 (6)
H2N—N1—H1N	105.0 (6)		

Symmetry codes: (i) −*x*+1, −*y*, −*z*+1; (ii) −*x*+1, −*y*+1, −*z*.

Hydrogen-bond geometry (Å, º)

D—H···*A*	*D*—H	H···*A*	*D*···*A*	*D*—H···*A*
O5—H5*A*···O4^{iii}	0.973 (7)	1.793 (7)	2.755 (4)	169.0 (7)
O5—H5*B*···O8^{iv}	0.997 (7)	1.656 (8)	2.642 (4)	168.9 (6)
O6—H6*A*···O3^{v}	0.981 (6)	1.722 (6)	2.696 (3)	170.8 (5)
O6—H6*B*···O4^{vi}	0.985 (6)	1.751 (5)	2.729 (3)	171.8 (7)
O9—H9*A*···O1^{vi}	0.979 (5)	1.732 (5)	2.707 (3)	173.8 (6)
O9—H9*B*···O2	0.966 (6)	1.895 (6)	2.811 (3)	157.2 (6)
O10—H10*A*···O3^{v}	0.977 (8)	1.740 (8)	2.713 (4)	173.0 (7)
O10—H10*B*···O2^{ii}	0.979 (6)	1.811 (7)	2.745 (4)	158.5 (7)
O11—H11*A*···O2^{vii}	0.966 (6)	1.772 (6)	2.726 (3)	168.6 (6)
O11—H11*B*···O1	0.966 (6)	1.824 (6)	2.750 (3)	159.5 (7)
C2—H2*A*···O2^{vii}	1.085 (6)	2.682 (9)	3.351 (4)	119.4 (6)
C2—H2*A*···O5^{viii}	1.085 (6)	2.716 (8)	3.489 (3)	127.9 (6)
C2—H2*B*···O10	1.091 (7)	2.579 (8)	3.649 (4)	166.7 (7)
N1—H1*N*···O7^{viii}	1.033 (7)	1.853 (7)	2.848 (3)	160.8 (7)
N1—H2*N*···O4	1.027 (8)	1.961 (7)	2.877 (3)	147.0 (7)
N1—H3*N*···O6	1.022 (6)	2.216 (7)	3.066 (3)	139.5 (5)

Symmetry codes: (ii) −*x*+1, −*y*+1, −*z*; (iii) −*x*, −*y*+1, −*z*+1; (iv) *x*−1, *y*, *z*; (v) *x*+1, *y*−1, *z*; (vi) *x*, *y*−1, *z*; (vii) *x*+1, *y*, *z*; (viii) −*x*+1, −*y*+1, −*z*+1.